Civil Engineering Infrastructures Journal, 53(1): 173 – 188, June 2020
Print ISSN: 2322-2093; Online ISSN: 2423-6691
DOI: 10.22059/ceij.2020.282153.1587

Discrete Element Modeling of Dynamic Compaction with Different Tamping Condition

Ghassemi, A.[1*] and Shahebrahimi, S.S.[2]

[1] Assistant Professor, Civil Engineering Department, Qazvin Branch, Islamic Azad University, Qazvin, Iran.
[2] M.Sc. Graduate, Civil Engineering Department, Qazvin Branch, Islamic Azad University, Qazvin, Iran.

Received: 26 May 2019; Revised: 14 Mar. 2020; Accepted: 13 Apr. 2020

ABSTRACT: Dynamic Compaction (DC) is a common deep compaction method that is usually used for densification of coarse-grained soils. Although traditional continuum-based models such as the Finite Element Method can be successfully applied for assessment of stress distributions or deformations induced by DC, they are typically not adequate for capturing the grain scale mechanisms of soil behavior under impact. In contrast, numerical models such as Discrete Element Method (DEM) in which the interaction of constituting distinct elements is explicitly simulated are promising for simulation of DC process. In this study, dynamic compaction in a dry rockfill was simulated through a two-dimensional DEM model. Based on the developed model, a series of analyses with various tamper weights and drop heights were conducted to investigate the effects of important factors such as energy and momentum per drop on DC results. Comparison of the obtained results with experimental observations reveal the capability of DEM for simulation of DC. The numerical simulations also confirm the positive effect of using conical-based tampers in DC process.

Keywords: Discrete Element Method, Dynamic Compaction, Tamper Shape.

INTRODUCTION

Dynamic compaction (DC) is a widespread soil improvement method that is commonly used for densification of granular soils by repeated dropping of a heavy tamper from considerable height in a pre-determined pattern on the ground. The mass of tamper generally ranges from 5 to 30 tons and drop height ranges from 10 to 30 m. Tamper is normally a flat based cylinder concrete or steel weight. After each tamper impact, compression waves, shear waves and surface waves are introduced into the soil mass. Compression and shear waves are principally responsible for soil densification. Shear waves with a smaller portion of the total compaction energy cause shear displacement and re-arrangement of the soil particles. Therefore, modification of tamper base can increase the energy transferred by shear wave and consequently improve the efficiency of DC.

Feng et al. (2000) evaluated the use of conical-based tamper to improve the efficiency of dynamic compaction using physical models. Their results showed that using 90^0 apex angle conical-based tampers

* Corresponding author E-mail: a_ghassemi@qiau.ac.ir

provide better DC efficiency than flat based tampers in the Mai-Liao sand, but to provide similar performance in the Ottawa sand. Experimental study by Arslan et al. (2007) confirmed the positive effect of conical-based tamper on the efficiency of dynamic compaction.

Nazhat and Airey (2012) examined flat, conical, shell and convex shaped tampers for dynamic compaction of two different soil. Their results showed that there are significant differences in the extent and magnitude of the compacted zone at depth; however, they concluded that no single tamper shape performed well across both investigated soil types. Recently, Mehdipour and Hamidi (2017) employed finite element method for simulation of dynamic compaction using flat and conical base tampers with various cone angles. Their results for different initial relative densities indicated that decrease in apex angle of conical tampers increases the improvement depth and conversely result in decrease in lateral influence of dynamic compaction.

Various numerical approaches including analytical solutions (Ardeshir et al., 2013) and continuum-based numerical models using advanced constitutive laws (Ghassemi et al., 2010; Ghanbari and Hamidi, 2014) have been proposed to investigate the ground response to impact loads. Although the conventional continuum-based models such as Finite Element models can be successfully applied for simulation of stress distribution or deformation of soil mass beneath foundation under dynamic load, they are typically not adequate for capturing grain scale mechanisms of soil behavior under impact. For example, porosity that is a primary parameter to evaluate the compaction of granular soil is difficult to be analyzed using continuum mechanics framework (Ma et al., 2015).

Particle-based methods such as Discrete Element Method (DEM) in which soil particles are represented by distinct elements and the interaction between particles is simulated explicitly are promising tools for simulation of DC process. Analysis of contact between interacting particles that is a key stage in numerical simulation by Discrete Element enables a robust modeling of tamper impact on the ground by DEM. Also, the particle-based nature of this method permits the porosity variations within the soil to be precisely followed during compaction process. It should be noted that, despite its merits, DEM is still not extensively used for practical engineering problems. The main reason can be primary attributed to high computational cost of considering a huge number of particles especially if irregular particle shape and advanced contact laws are considered.

Following the pioneer study by Cundall and Strack (1979), the DEM has been developed with applications in various fields of engineering such as geotechnical engineering (Wei and Wang, 2006), petroleum engineering (Cui et al., 2016), mining engineering (Xu et al., 2016) and powder engineering (Garner et al., 2018). In DEM, the properties of an assembly of rigid particles under loading such as position and velocity of individual particles and contact forces between particles are updated at every time step. The translational and rotational displacements of each particle are calculated by integrating the differential equations of the motion based on Newton's second law. The contact forces between particles are obtained using pre-defined force–displacement contact models. Therefore, the interactions between particles and the displacements of each individual particle can be traced in DEM process.

Despite such an approach appears to be appropriate for numerical simulation of soil behavior under impact load, only a few

recently developed DEM models have been employed for numerical simulation of DC process. Since modeling of full scale 3D problems using particle-based methods such as DEM requires applying extremely high capacity computational resources, these studies are mainly consisting of modeling of DC at small scales and the focus of such researches is mostly on the investigation of micro-mechanisms involved in DC process. Wada et al. (2006) modeled the tamper impact on a granular material using a 2D discrete element method.

Numerical simulations of the low energy dynamic compaction in gravelly soil ground were studied by Ma et al. (2014). They used a dynamic hysteretic contact model to incorporate the dynamic hysteresis effect. Their study indicated that the reduction in porosity of the granular soil under impact loading depends on the values of the contact stiffness of the soil particles. In a later study, numerical simulations of DC process in gravelly soil ground and soil-structure interaction near a bridge foundation were investigated via DEM by Ma et al. (2015). They concluded that dynamic horizontal pressure on the bridge foundation estimated by DEM is smaller than that of obtained by the continuum-based numerical model.

Recently, DEM was utilized by Jiang et al. (2016) utilized for simulation of dynamic compaction. The focus of their study was on investigating the effect of viscous damping coefficient on compaction under various tamping energy. This study showed that rebound of the tamper increases with the decreasing damping coefficient. None of the abovementioned studies used DEM to achieve real scale results comparable to field measurements or empirical relationships. In a recent study, Jia et al. (2018) implemented coupled Discrete Element- Finite Difference method to simultaneously disclose the macro and micro mechanisms involved in dynamic compaction of granular soils in real scale.

In this study, dynamic compaction in dry rockfill is simulated through DEM in two dimensions using PFC2D (Itasca, 2014). In contrast to previous DE studies in which circular (or spherical) tampers have been modeled, dropping of flat based tamper which is more usual in DC treatments is considered in this study. Based on the developed model, a series of analyses with various tamper weights, drop heights and number of drops are conducted to investigate the effects of important factors such as energy and momentum per drop on DC results. Furthermore, the effects of using conical tampers with different cone apex angles on crater depth and depth of improvement are investigated by the developed model.

DISCRETE ELEMENT METHOD

Discrete element method (DEM) is an explicit numerical approach for simulation of the behavior of a medium comprising of an assembly of rigid distinct particles. Rigid particles can interact with each other or with solid walls where overlap between particle/particle or particle/wall occurs. The contact forces can be related to the magnitude of the overlaps by using an appropriate contact-force displacement law. The displacement and velocity of each individual solid particle are calculated from the summation of all forces and moments acting on the particle using Newton's second law of motion. This calculation cycle is repeated in each time step during the numerical analysis (Ghassemi and Pak, 2015).

In this study, the Hertz contact model consists of a nonlinear Hertzian component based on an approximation of the theory of Mindlin was applied. In this model, the normal contact force (F_n) in each time step has a nonlinear relationship with normal particles overlap (δ_n) as (Itasca, 2014):

$$F_n = h_n \left| \delta_n \right|^{1.5} \quad (1)$$

The coefficient h_n: depends on the geometrical and mechanical properties of the contacting pieces as (Itasca, 2014):

$$h_n = \frac{2G\sqrt{2\overline{R}}}{3(1-\upsilon)} \quad (2)$$

where G and υ: are shear modulus and Poisson's ratio of particles, relatively and $\overline{R}$: is the harmonic average of radii of two contacting particles.

Shear contact force at each time step is updated as follows:

$$F_t = F_{t0} + k_t \Delta\delta_t \quad (3)$$

where F_{t0}: is the Hertz shear force at the beginning of the time step and $\Delta\delta_t$: is the relative shear increment in the same time step. In this equation, k_t: is the tangent shear stiffness, which depends on the current normal force as (Itasca, 2014):

$$k_t = \frac{3(1-\upsilon)}{2-\upsilon} h_n (F_n)^{\frac{1}{3}} \quad (4)$$

Also, for further energy dissipation in simulation of impact of tamper on the ground, viscous dashpots considered to be added to the Hertz normal contact force (Itasca, 2014):

$$F_n^d = 2\beta_n \sqrt{m_c k_n}\, \dot{\delta}_n \quad (5)$$

where β_n: is the normal critical damping ratio and $\dot{\delta}_n$: is the relative shear translational velocity. k_n: is the normal tangent stiffness that can be simply derived from Eq. (1). m_c: is effective mass of two contacting particles ($m_c = m_1 m_2/(m_1 + m_2)$).

The tangential contact forces are usually governed by frictional relationships. The Coulomb friction criterion was employed in this study. Accordingly, the commencement of slippage occurs where the tangential contact force exceeds the following criterion:

$$(F_{t,j})_{\max} = \mu_s F_{n,j} \quad (6)$$

where μ_S: is the sliding friction coefficient between two contacting solid particles and $F_{n,j}$ and $F_{t,j}$: are the normal and tangential contact forces on particle j.

The non-viscous local damping approach was used to simulate damping force ($F_{nv,ij}$) and moment ($M_{nv,j}$):

$$F_{nv,ij} = -\alpha \left| F_{ij} \right| sign(\dot{x}_{ij}) \quad (7)$$

$$M_{nv,j} = -\alpha \left| M_j \right| sign(\dot{\theta}_j) \quad (8)$$

where F_{ij} and M_j: are the unbalanced force (at direction i) and unbalanced moment on particle j, a: is non-viscous damping coefficient, $\dot{x}_{ij}$: is linear velocity of particle j at direction i, and $\dot{\theta}_j$: is angular velocity of particle j.

In DEM, the relationship between the applied forces and moments and the movement of particles is defined based on the Newton's second law of motion. The 2D form of this law was applied in this study:

$$m_j \ddot{x}_{ij} = \sum F_{ij} \quad (9)$$

$$I_j \ddot{\theta}_j = \sum M_j \quad (10)$$

where $\ddot{x}_{ij}$ and $\ddot{\theta}_j$: are linear and angular accelerations of particle j at direction i and m_j and I_j: are the mass and moment of inertia of discrete particle j, respectively.

NUMERICAL MODEL

Material

In this study, dynamic compaction of dry rockfill material was considered. Although field studies indicate that DC is an economical solution for compaction of loose rockfill material, reliable experimental or numerical studies can be rarely found in the literature. Besides, due to high computational cost of simulation by discrete element method, modeling of rockfill provides the chance of simulation of real DC problem using such grain scale method. For this purpose, circle rigid particles with average size of 50 mm were generated to prepare the loose rockfill ground. The mechanical behavior of the rockfill material depends on its particle size distribution (gradation). In this study, the Weibull distribution, which is a continuous probability distribution function was employed to create the desired particle size distribution:

$$f(D) = 1 - e^{-(\frac{D}{Dw})^n} \quad (11)$$

where Dw: is the particle diameter that 63.2% of particles are finer than it, and n: is a constant which specifies the flatness of the distribution. The lower the constant n, the more non-uniform is the particle size distribution. For instance, $n \to \infty$ represents mono-sized particulate systems. In this work, gradation curve of rockfill was created by the Weilbull distribution function using D_w = 50 mm and n = 20 represent a well graded soil (continuous curves in Figure 1). For numerical simulations, a few sizes from the created gradation curve (15, 30, 50 and 80 mm) were selected. The selected sizes are shown on the curves by using special symbols. Based on this gradation, the ratio of tamper width to the average particle size is around 60. Yang et al. (2007) conducted a number of centrifuge tests to investigate the particle size effects on bearing capacity of a circular footing in sandy ground. They concluded that when the ratio of model footing diameter to particle size is more than 50, the ultimate bearing capacity of the prototype footing is independent of the diameter of model footing for the cases that footing constructed on the ground surface. Regarding the analogy between load transfer mechanism in DC with flat based circular tamper and bearing capacity of circular footing rested on the ground surface, the ratio of tamper width to the average particle size in this study is reasonable.

All parameters used for DEM analyses of the ground under dynamic compaction process are presented in Table 1. For conducted DEM analyses, the number of generated particles were about 140,000. The values considered for density and Poisson's ratio are within the typical range for these parameters. A series of analyses were conducted with different values for shear modulus, non-viscous damping coefficient and sliding friction coefficient. The numerical results were compared to the field tests to choose proper values. The results showed that non-viscous damping (α) coefficient has not significant effect on the depth of improvement. However, increasing in shear modulus leads to decrease in both improvement depth and crater depth. The details of these analyses can be found elsewhere (Shahebrahimi, 2018).

Table 1. DEM parameters

Parameter	Value
Number of particles	~140,000
Diameter (mm)	15, 30, 50, 80
Density (kg/m^3)	2600
G (MPa)	1000
υ	0.2
μ_S	0.3
α	0.7
β_n	0.3

Critical damping ratio (β_n), which represents the viscous damping, is closely related to the coefficient of restitution. The coefficient of restitution (ε) is defined as the ratio of impact velocity to rebound velocity. If ε = 1 the impact is perfectly elastic, if ε = 0 the impact is totally inelastic (Teufelsbauer et al., 2009). Jiang et al. (2016) concluded that an inappropriate value for viscous damping would result in unreasonable rebound of falling tamper. Roesset et al. (1994) proposed a value of 1/3 for the problem of impact of weight falling onto the ground. The equivalent normal critical damping ratio (β_n = 0.3) was applied in this study.

Ground Preparation

The important step in modeling of ground by DEM is providing a stable assembly of contacting particles under gravity. The most used method for generation of assemblies in DEM is particle filling procedure. This approach includes sequentially selecting of particles according to a given particle size distribution in descending order of size and creating random coordinates to position them within a pre-defined domain. This approach was employed in this study.

To ensure that no overlap exists between the new created particle and previously created particles in the domain, positioning of each solid particle may need to repeated a number of times till the new particle is positioned correctly. In each trial, if new created particle has overlap small with a neighboring particle, a small change in the coordinates is applied to the particle which may lead to removal of the overlap. The coordinate change is repeated a number of times to eliminate all existing overlaps. If these attempts do not work, a new random coordinates are allocated to the particle. In this study, the random coordinate generation continued up to 5×10^5 times.

Particle filling procedure is only useful for generating very loose samples in which individual particles are not in contact with neighboring particles. Therefore, gravity sedimentation of the randomly generated assembly was considered to form the ground in the DEM model. For this purpose, the generated particles were released under gravitational acceleration in a domain enclosed by right, left and bottom rigid boundary walls. As a result, the particles fell to the bottom of the space and gradually form the soil layers. In this stage, low value friction coefficient causes the particles slide more freely over each other, and consequently a dense packing will be created. Conversely, large friction coefficient generates looser samples.

Other approaches such as radius growing method (Itasca, 2014) are also available which are able to create more homogenous packing, but with more computational complexities. It should be noted that the dimension of the domain should be considered large enough so that the effects of boundaries on compaction process is limited. In this study, the appropriate dimension of the model was selected to be 12 m depth by 16 m width after some trial and error. Beyond these dimensions, the porosity reduction due to compaction effect of impacts is less than 0.5%.

Simulation of Impact

In the finite element context, modeling of tamper impacts on the ground is always a difficult task. In contrast, in DEM simulations, the tamper is released from a desired height of drop, simply by applying gravity to tamper element in the numerical model. This is closely to what occurs during free fall dynamic compaction in the field. After each impact, the acceleration of the tamper diminishes rapidly until the tamper stops. At this instant, the tamper is moved back to its initial position in numerical model

for simulation of the next drop. Snapshots of modelled falling flat base tamper are shown in Figure 2.

Geometrical characteristics of tampers significantly affects the results of dynamic compaction. A number of approaches have been proposed in the literature to address the issue of non-circular elements modeling in DEM simulations. One class of methods relies on approximating the non-circular shapes using polygons (e.g. Hosseininia, 2016). Another approach is to combine several non-overlapping circular particles into a rigid cluster to form a non-circular element (Boutt and Mcpherson, 2002). Since only non-overlapping circular discs are used within each cluster, the simulated geometries do not resemble sharp corners of angular elements efficiently.

Another approach is based on clump logic that relies on clumping a number of overlapping disk elements to best represent a non-circular element. The number of overlapping circles, which represent the non-circular element, depends on the degree of non-uniformity in shape, angularity of the particle and the desired level of geometric accuracy. The clump logic has been extensively used for numerical simulation of irregular shaped particles. Further, this technique has been applied for simulation of solid objects interacting with soil particles (Wang, 2016; Syed et al., 2017).

The clump logic was utilized in current study using 60 overlapping circles to adequately capture the shape of flat based tamper with 2.5 m tamper diameter. Because the tamper contains a number of overlapping circular particles, the density of particles must be scaled to ensure the desired mass and moment inertia of the tamper. In this study, the tamper weight ranges from 10 to 30 tons and the height of dropping is in the range of 5 to 25 m. Five to ten drops in each compaction point were applied in various analyses.

Assessment of Compaction

Figure 3 shows a snapshot of the model after first impact. The color level for the particles in Figures 3a and 3b illustrates the x- and y- components of particle velocity vectors, respectively. The semi-circular compaction wavefront can be distinguished in this figure. In Figure 3a, both black and white colors indicate high values of x-component of particle velocity but in two opposite directions. In Figure 3b, the magnitude of y-velocity is shown by a range of colors from white to black which implies low to high magnitude, respectively.

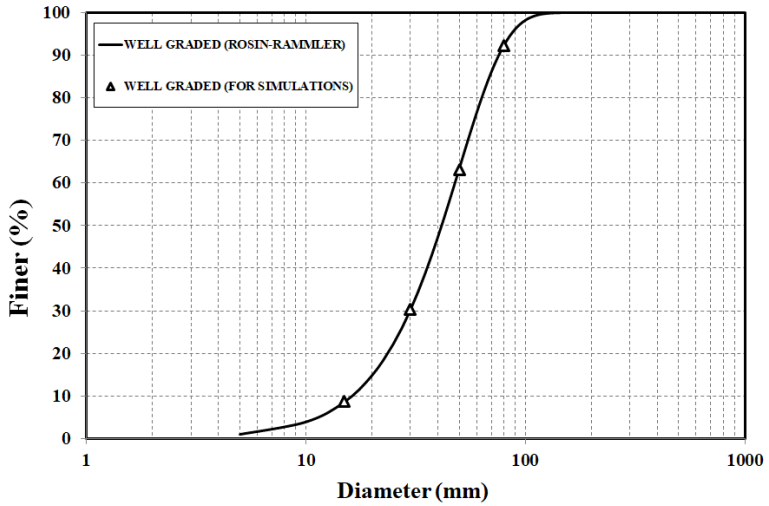

Fig. 1. Particle size distribution curve used in this study

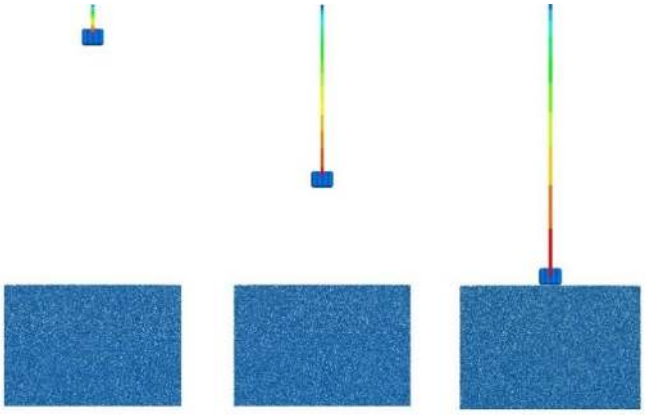

Fig. 2. Snapshots of modelled free falling tamper (left to right)

Relatively large downward/small lateral particle velocities beneath the centerline of the impact imply a K_0 compression state which can be attributed to lateral inertia of surrounding soil. At farther distance, the pattern of particles movement changes to biaxial condition. White colored particles close to the impacted tamper indicate upward movement of particles that can result in loosening of the surface soil. It should be noted that surface deposits are usually expected to be loosened to the depth of crater penetration as result of DC (Lukas, 1995).

Densification of soil under impact loads can be easily evaluated via porosity reduction of the soil mass. In DEM, porosity in a small region of the assembly is usually calculated by defining a circle (measurement circle) bounding the individual particles in that region. For two-dimensional problems, the porosity of the assembly (n) is defined as the ratio of the total void area (A_v) within the measurement circle (instead of volume) to total area of the circle (A_c):

$$n = \frac{A_V}{A_C} \tag{12}$$

However, the values of porosity in 2D analyses is not necessarily equivalent to physical porosity of soil mass as defined in soil mechanics. Therefore, in this study, the ratio of porosity reduction to initial porosity (Δ_n/n_0) was employed as the key parameter for investigation of DC improvement effects.

Two rows of measurement circles with 2.0 m diameter were provided for tracing the variation of porosity in depth beneath the tamper and laterally from impact point. Therefore, the ratio of measurement circle diameter to the mean particle size is 40. Based on numerical results, fairly good agreement among porosities from different measurement circles was observed. The variation of Δ_n/n_0 with time (after impact) in different depth beneath the compaction point under first impact of flat base tamper is shown in Figure 4. As can be seen in this figure, during the impact, Δ_n/n_0 in each depth increases to a very high value as the body waves pass through the point and then reduces to a lower value over the impact period. It can be observed on the figure that, the final value of Δ_n/n_0 gradually decreases as the depth increases. For this case (dropping of 20 t tamper from height of 15 m on poorly graded ground), the increase in Δ_n/n_0 becomes very small at depth 5.6 m.

Improvement (or influence) depth is the most important factor in the process of DC design. In DC literature, improvement depth is normally defined as the maximum depth that is affected by compaction and improvement beyond that depth is negligible (Slocombe, 2004). Several researchers have

attempted to propose a quantitative definition of improvement (Ghassemi et al., 2009). In DEM analysis, the depth of improvement should be expressed in terms of porosity. In this study, the depth of improvement is defined as a depth beyond which increase of Δ_n/n_0 values is less than 5%. For example, the improvement depth for the case shown in Figure 5 is calculated to be around 6.3 m after three impacts. It should be noted that in the practice, the improvement depth is normally measured after all impacts are dropped at a compaction point.

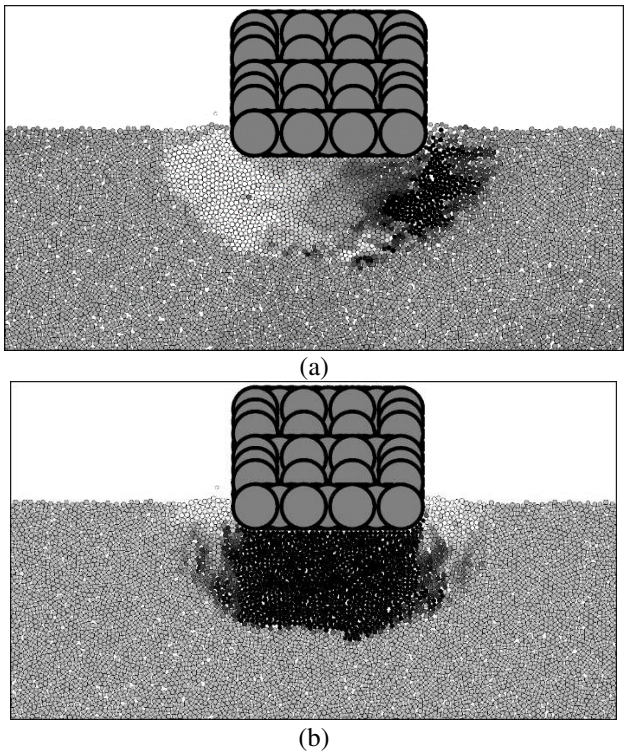

(a)

(b)

Fig. 3. A snapshot of the model after first impact: a) black and white colors indicate higher values of x- velocity in two opposite directions; b) changes from white to black implies low to high magnitude the magnitude of y-velocity

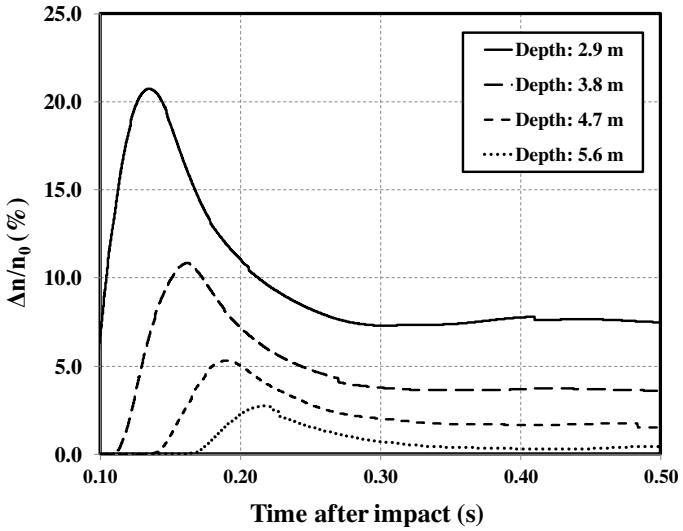

Fig. 4. Variation of the ratio of porosity reduction to initial porosity over time at different depths

As can be seen in Figure 5, the overall degree of improvement increases by number of impacts; however, the compaction effect decreases as the impacts progress. Also, the numerical results indicate that the average improvement is less than the maximum amount that occurs at a depth of around 4.0m. It is in agreement with field measurements that yield this depth between 1/3 to 1/2 of the maximum depth of influence (Lukas, 1995). Improvement effect in lateral direction obtained by the first three impacts at 2 m depth is depicted on Figure 6. The figure imply that the lateral expansion of compaction noticeably diminishes with the distance from center of tamping.

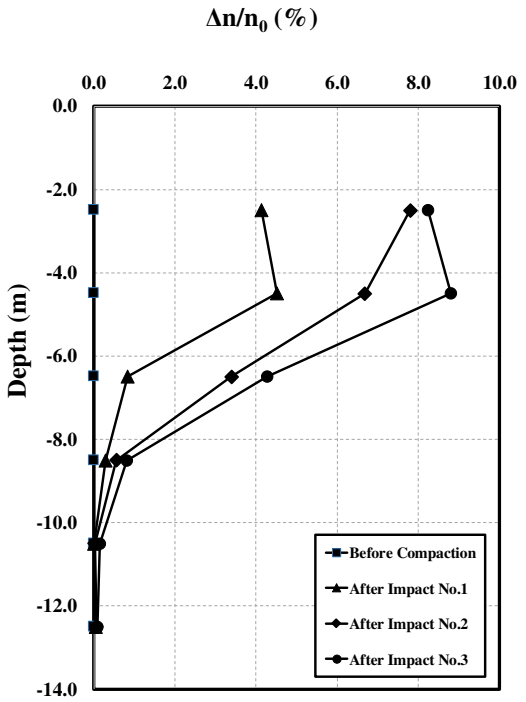

Fig. 5. Variation in improvement with depth during first three impacts

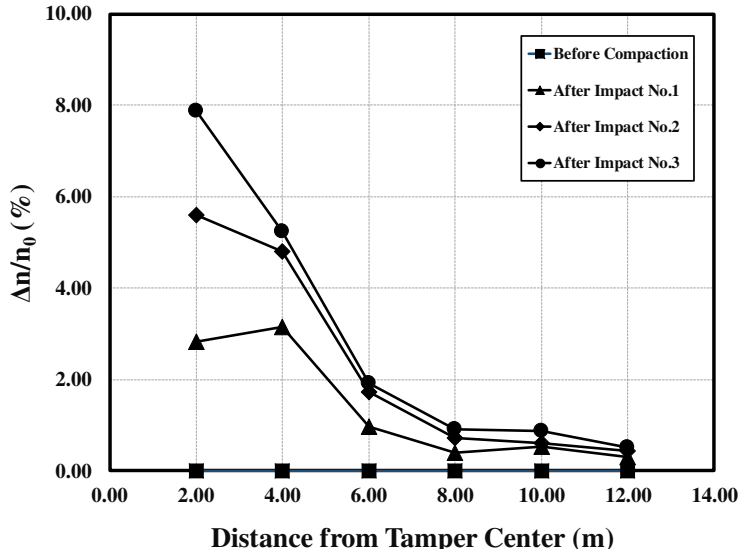

Fig. 6. Variation in improvement in lateral direction during first three impacts

EFFECTS OF IMPACT ENERGY AND MOMENTUM

The well-known Menard's formula for predicting depth of improvement in DC treatment which was originally proposed by Menard and Broise (1975) and later adapted by others (Mayne et al., 1984; Lukas, 1995) is as follows:

$$DI = n\sqrt{WH} \tag{13}$$

where *DI*: is the depth of improvement (m), *W*: is weight of tamper (ton) and *H*: is falling height (m). The empirical coefficient *n* that depends on numerous factors such as soil type and degree of saturation (Lukas, 1995) varies between 0.3 and 0.8 (Mayne et al., 1984).

This simple and relatively accurate formula have been widely used by DC practitioners (Ghassemi et al., 2009). However, as the source of energy in DC is located at the ground surface, the linear trend especially for higher dropping energies is under question. Slocombe (2004) proposed a threshold energy that the using higher energies beyond it, is not effective to reach deeper improvement depths. This issue was also confirmed by numerical studies using FEM (e.g. Ghassemi et al., 2009). To study the problem by discrete element method, the results of some of the analyses with flat base tamper for are presented in Figure 7. The figure shows that variation of the improvement depth with the square root of energy per drop predicted by the numerical model is in agreement with Slocombe (2004). By inspecting the numerical data depicted on Figure 7, one can discover that the improvement depth can be significantly different even if same energy is applied to densify (see data symbols related to 150 tm energy per drop).

It has been proven that momentum of impact has a significant effect on dynamic compaction results. Momentum of impact is the product of the mass (*W*) and velocity of the tamper at the instant of impact (V_{impact}) which is equal to $WV_{impact} = W\sqrt{2gH}$. Based on a series of centrifuge tests, Oshima and Takada (1997) showed that depth of the compacted zone has almost linear relation with the logarithm of the total momentum of all drops during DC. Their proposed relation has been plotted in Figure 8. Numerical results of this study were also added to the chart. As can be seen in Figure 8, the DEM results confirm the dependence of improvement depth on total momentum of impacts and despite the two-dimensionality of the numerical model, the results are in agreement with the trends of the proposed lines based on centrifuge test results.

EFFECTS OF TAMPER BASE SHAPE

In this study, flat based and conical based tampers with cone angles of 60°, 90° and 120° were considered. For all tampers, the height and diameter of the tampers are 1.5 m and 2.5 m, respectively (see Figure 9). For each tamper shape, a series of analyses with various tamper weights, drop heights and number of drops were conducted. The density of tamper material was adjusted to preserve a same weight for all tamper base shapes. The results show that using different tamper shape considerably affects the induced crater depth and depth of improvement.

a) Crater depth: One of the most obvious manifestation of the DC process is the relatively large craters created due to impact of heavy falling weights in compaction points. The increase of crater depth with increasing the number of impacts is a simple sign of the continuing improvement process. Mayne et al. (1984) analyzed the field measurements of over 120 sites to investigate the response of the ground to DC. The result of this study indicated that when the

measured crater depths are normalized with respect to the square root of energy per drop, the data fall within a relatively narrow band. However, there are some observations indicating that crater depth has a linear relation with the square root of drop counts (Takada, 1994).

In Figure 10, the results of numerical simulation of DC with different shape of tamper base are compared to those analyzed by Mayne et al. (1984) adapted from a number of DC sites with the similar applied energy per drop. The linear trend can be observed in both the numerical and the experimental results. The fitted line to the numerical results of flat base tamper falls within the data adapted from DC projects that imply the capability of the DE model to simulate the trend of crater depth increase with number of drops. The fitted lines to numerical results obtained from analysis of tamping of conical base weight on the ground are also added to this figure. As can be seen, by increase of the cone angle both the slope and interception of fitted lines decreases. The higher normalized crater depth for sharper angles might be considered as a sign of tamper punching into the ground that would reduce the improvement effect of DC.

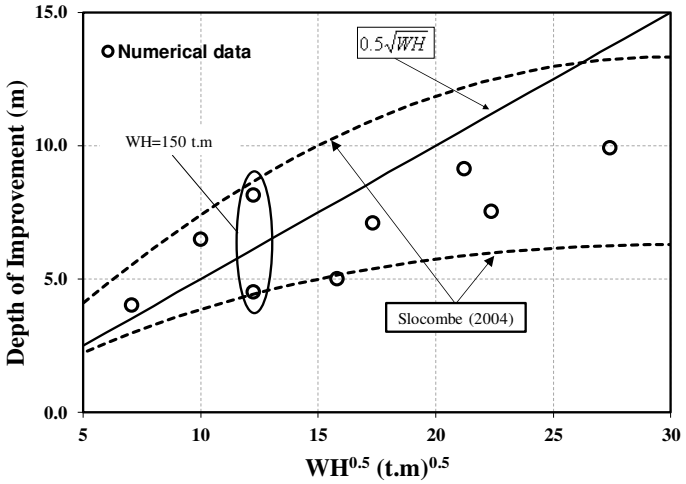

Fig. 7. Relation between depth of improvement and square root of applied energy per drop

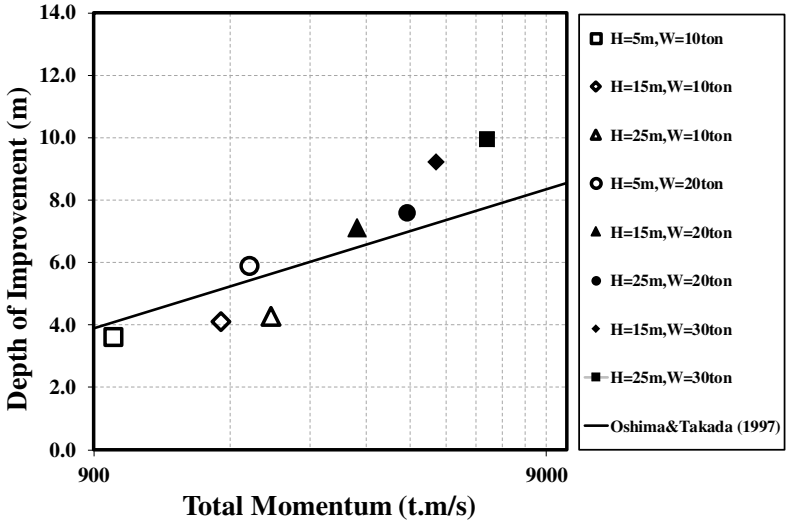

Fig. 8. Relation between depth of improvement and the logarithm of the total momentum

b) Depth of improvement: The efficiency of using conical tampers with different cone angles over a range of applied energy per drops was shown in Figure 11. The vertical axis is the ratio of increase in improvement depth obtained by conical base tampers to the improvement depth of flat base tamper with the same weight and base diameter. From this figure, the numerical simulations confirm the positive effect of using conical base tampers on improvement depth of DC. As mentioned earlier, tamper punching into the ground, which results in reduction in improvement depth, is more likely to occur when conical tamper is used.

On the other hand, using conical tampers can increase the DC efficiency by introducing more energy through shear wave propagation. Based on numerical results, it seems that the resultant of these two opposite mechanisms is increase in depth of improvement when conical tamper is applied. However, the amount of effectiveness depends on the cone angle and applied energy per drop. Although the decrease of cone angle from 120 to 90 results in significant increase in depth of improvement especially for intermediate values of applied energy per drop, less positive effect is obtained by changing cone angle from 90 to 60.

Also, the figure shows that the largest depth of improvement for all analyzed tamper bases is achieved with neither the smallest nor the largest energy per drop, consequently, it offers an optimum value of energy per drop while conical shaped tampers are applied. Since the base area of all tampers are the same for all analyses, increase of applied energy could result in punching of conical tampers into the ground without further improvement. It is worth mentioning that using too small tamper base diameter may also cause a similar effect of less improvement depth due to occurrence of punching (Ghassemi et al., 2009).

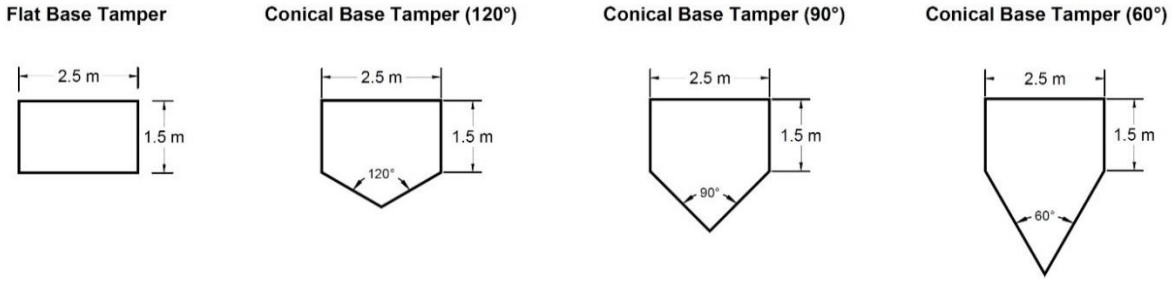

Fig. 9. Tampers with different base shapes considered in this study

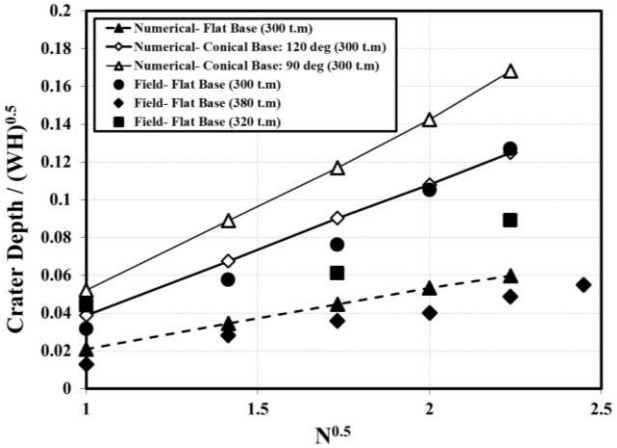

Fig. 10. Relation between normalized crater depth and square root of drop counts

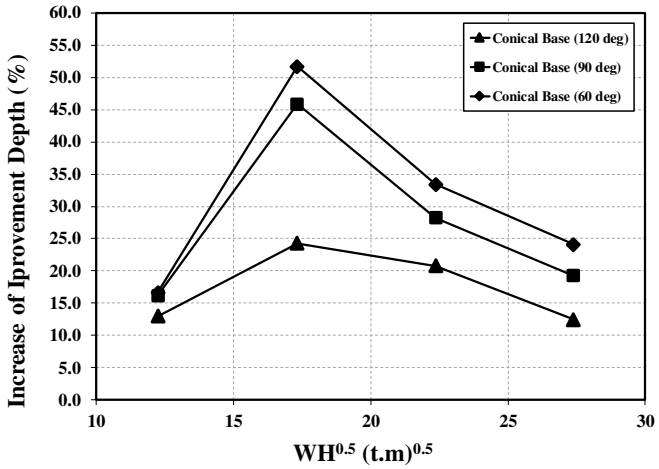

Fig. 11. Increase in improvement depth due to using conical base tampers for different applied energy per drop

CONCLUDING REMARKS

In this study, Discrete Element Method (DEM) has been employed for simulation of the Dynamic Compaction (DC) on dry loose rockfill ground. The particle-based nature of DEM provides an appropriate framework to track the variation of porosity as the key parameter representing the soil compaction process. Also, in DEM simulations, the tamper can be released from a desired drop height simply by applying gravity to the tamper, similar to what occurs during free fall DC in the field. In the developed numerical model, clump logic that relies on clumping a number of overlapping disk elements to represent a non-circular element was applied to adequately capture the shape of both flat and conical based tampers. The obtained results show the capability of the DEM model to investigate the effects of important influencing factors including applied energy and momentum of drops as well as the effects of using different tamper base shapes on crater depth and depth of improvement. Based on the obtained results, the following conclusions can be drawn:

• The numerical results indicate that for heavier tampers and higher energy per drops, the Menard formula which predicts a linear relation between improvement depth and energy per drops overestimates the depth of improvement. This is in agreement with previous field and numerical studies.

• Previous experimental and numerical studies have proved that for a same level of energy per drop, dropping heavier tamper from less falling height increases the depth of improvement. The DEM results confirm the dependence of improvement depth on total momentum of impacts and the results are in agreement with the trends proposed based on centrifuge test results.

The results of this study also reveal that using different tamper shape affects the induced crater depth and depth of improvement:

• The numerical results confirm the linear trend between the normalized crater depth (crater depth/ energy per drop) with the square root of drop number for all examined tamper base shapes. However, sharper angles of tamper base results in increase of both the slope and interception of the fitted lines that might be considered as a sign of tamper punching into the ground.

• The numerical simulations confirm the positive effect of using conical base tampers on improvement depth of DC. The amount of effectiveness depends on both the cone angle

and the applied energy per drop. The results imply that the largest depth of improvement is achieved with neither the smallest nor the largest energy per drop, consequently, it offers an optimum value of energy per drop while conical shaped tampers are applied.

Despite some limitations of the model, such as its two-dimensionality and idealization of soil grains by circular rigid particles, this study shows that the Discrete Element Method can capture the key issues that are involved in the behavior of granular ground under impact of tampers with different base shapes. Numerical modeling in three-dimensional domain and simulation of the interaction between irregular shape particles is the future work of this research program.

REFERENCES

Ardeshir, B.A., Eskandari, G.M. and Vaseghi, A.J. (2013). "Analytical solution for a two-layer transversely isotropic half-space affected by an arbitrary shape dynamic surface load", *Civil Engineering Infrastructures Journal*, 46(1), 1-14.

Arslan, H., Baykal, G. and Ertas, O. (2007). "Influence of tamper weight shape on dynamic compaction", *Proceedings of the Institution of Civil Engineers-Ground Improvement*, 11(2), 61-66.

Boutt, D. and McPherson, B. (2002). "The role of particle packing in modeling rock mechanical behavior using discrete elements", In: *Discrete Element Methods: Numerical Modeling of Discontinua,* 86-92.

Cui, Y., Nouri, A., Chan, D. and Rahmati, E. (2016). "A new approach to DEM simulation of sand production", *Journal of Petroleum Science and Engineering,* 147, 56-67.

Cundall, P.A. and Strack, O.D. (1979). "A discrete numerical model for granular assemblies", *Geotechnique*, 29(1), 47-65.

Feng, T.W., Chen, K.H., Su, Y.T. and Shi, Y.C. (2000). "Laboratory investigation of efficiency of conical-based pounders for dynamic compaction", *Geotechnique*, 50(6), 667-674.

Garner, S., Strong, J. and Zavaliangos, A. (2018). "Study of the die compaction of powders to high relative densities using the discrete element method", *Powder Technology*, 330, 357-370.

Ghanbari, E. and Hamidi, A. (2014). "Numerical modeling of rapid impact compaction in loose sands", *Geomechanics and Engineering*, 6(5), 487-502.

Ghassemi, A. and Pak, A. (2015). "Numerical simulation of sand production experiment using a coupled Lattice Boltzmann–Discrete Element method", *Journal of Petroleum Science and Engineering*, *135*, 218-231.

Ghassemi, A., Pak, A. and Shahir, H. (2009). "Validity of Menard relation in dynamic compaction operations", *Proceedings of the Institution of Civil Engineers-Ground Improvement*, 162(1), 37-45.

Ghassemi, A., Pak, A. and Shahir, H. (2010). "Numerical study of the coupled hydro-mechanical effects in dynamic compaction of saturated granular soils", *Computers and Geotechnics*, 37(1-2), 10-24.

Hosseininia, E.S. (2016). "On the Stress-Force-Fabric relationship in anisotropic granular materials", *International Conference on Discrete Element Methods,* Springer, Singapore, 475-483.

Itasca, C.G. (2014). "PFC (Particle Flow Code in 2 and 3 dimensions), version 5.0, User's manual", *Numerical and Analytical Methods in Geomechanics*, 32(6), 189-213.

Jia, M., Yang, Y., Liu, B. and Wu, S. (2018). "PFC/FLAC coupled simulation of dynamic compaction in granular soils", *Granular Matter*, 20(4), 76.

Jiang, M., Wu, D. and Xi, B. (2016). "DEM simulation of dynamic compaction with different tamping energy and calibrated damping parameters", *International Conference on Discrete Element Methods*, Springer, Singapore, 845-851.

Lukas R.G. (1995). *Geotechnical engineering circular No. 1: Dynamic compaction*, No. FHWA-SA-95-037, United States. Federal Highway Administration. Office of Technology Applications.

Ma, Z.Y., Dang, F.N. and Liao, H.J. (2014). "Numerical study of the dynamic compaction of gravel soil ground using the discrete element method", *Granular Matter*, 16(6), 881-889.

Ma, Z., Liao, H., Ning, C. and Liu, L. (2015). "Numerical study of the dynamic compaction via DEM", *Japanese Geotechnical Society Special Publication*, 1(3), 17-22.

Mayne, P.W., Jones Jr, J.S. and Dumas, J.C. (1984). "Ground response to dynamic compaction", *Journal of Geotechnical Engineering*, 110(6), 757-774.

Mehdipour, S. and Hamidi, A. (2017). "Impact of tamper shape on the efficiency and vibrations

induced during dynamic compaction of dry sands by 3D Finite Element modeling", *Civil Engineering Infrastructures Journal*, 50(1), 151-163.

Menard, L. and Broise, Y. (1975). "Theoretical and practical aspects of dynamic consolidation", *Geotechnique*, 25(1), 3-18.

Nazhat, Y. and Airey, D.W. (2012). "The effect of different tamper geometries on the dynamic compaction of sandy soils", *International Symposium on Ground Improvement (IS-GI),*

Oshima, A. and Takada, N. (1997). "Relation between compacted area and ram momentum by heavy tamping", *Proceedings of the International Conference on Soil Mechanics and Foundation Engineering-International Society for Soil Mechanics and Foundation Engineering,* 3, AA Balkema, 1641-1644

Roesset, J.M., Kausel, E., Cuellar, V., Monte, J.L. and Valerio, J. (1994). "Impact of weight falling onto the ground", *Journal of Geotechnical Engineering*, 120(8), 1394-1412.

Shahebrahimi S.S. (2018). "Numerical simulation of dynamic compaction using Discrete Element method", M.Sc. Thesis, Islamic Azad University, Qazvin, Iran.

Slocombe (2004). "Dynamic compaction", In: Moseley, M.P. and Kirsch, K. (eds.), *Ground improvement*, CRC Press., 93-118.

Syed, Z.I. (2017). "Development and calibration of discrete element method inputs to mechanical responses of granular materials", Ph.D. Dissertation, Iowa State University.

Takada, N. (1994). "Comparison between field and centrifuge model tests of heavy damping", *Proceedings of International Conference on Centrifuge.*

Teufelsbauer, H., Hübl, J. and Wu, W. (2009). "A revision of the linear-dashpot model applied in PFC", *Contemporary Engineering Sciences*, 2(4), 165-178.

Wada, K., Senshu, H. and Matsui, T. (2006). "Numerical simulation of impact cratering on granular material", *Icarus*, 180(2), 528-545.

Wang, P. and Arson, C. (2016). "Discrete element modeling of shielding and size effects during single particle crushing", *Computers and Geotechnics*, 78, 227-236.

Wei, J. and Wang, G. (2017). "Discrete-element method analysis of initial fabric effects on pre-and post-liquefaction behavior of sands", *Géotechnique Letters*, 7(2), 161-166.

Xu, N., Zhang, J., Tian, H., Mei, G. and Ge, Q. (2016). "Discrete element modeling of strata and surface movement induced by mining under open-pit final slope", *International Journal of Rock Mechanics and Mining Sciences*, 88, 61-76.

Yang, J.J., Liu, F., Toyosawa, Y., Horiyi, N. and Itoh, K. (2007). "Particle size effects on bearing capacity of sandy ground in centrifugal tests", *Yantu Gongcheng Xuebao (Chinese Journal of Geotechnical Engineering)*, 29(4), 477-483.